HHS Public Access

Author manuscript

Biochemistry. Author manuscript; available in PMC 2017 October 26.

Published in final edited form as:

Biochemistry. 2016 November 15; 55(45): 6327–6336. doi:10.1021/acs.biochem.6b00932.

Curcumin inhibits PKCα activity by binding to its C1 domain

Satyabrata Pany, **Youngki You**, and **Joydip Das***

Department of Pharmacological and Pharmaceutical Sciences, College of Pharmacy, University of Houston, Houston, TX 77204

Abstract

Curcumin is a polyphenolic nutraceutical that acts on multiple biological targets, including protein kinase C (PKC). PKC is a family of serine-threonine kinases central to intracellular signal transduction. We have recently shown that curcumin selectively inhibits PKCα, but not PKCε in CHO-K1 cells (Pany, S. (2016) Biochemistry *55*, 2135–43). To understand which domain(s) of PKCα is/are responsible for curcumin binding and inhibitory activity, we made several domain-swapped mutants in which the C1 (combination of C1A and C1B) and C2 domains are swapped between PKCα and PKCε. Phorbol ester-induced membrane translocation studies using confocal microscopy and immune-blotting revealed that curcumin inhibited phorbol ester induced membrane translocation of PKCε mutants, in which εC1 domain was replaced with αC1, but not the PKCα mutant in which αC1 was replaced with εC1 domain, suggesting that αC1 is a determinant for curcumin's inhibitory effect. Further, curcumin inhibited membrane translocation of PKCε mutants, in which εC1A and εC1B domain were replaced with αC1A and αC1B domains, respectively, indicating the role of both αC1A and αC1B domains in curcumin's inhibitory effects. Phorbol 13-acetate inhibited curcumin binding to αC1A and αC1B with IC_{50} values of 6.27 μM and 4.47 μM, respectively. Molecular docking and molecular dynamics studies also supported higher affinity of curcumin for αC1B than αC1A. The C2 domain swapped mutants were inactive in phorbol ester induced membrane translocation. These results indicate that curcumin binds to the C1 domain of PKCα and highlight the importance of this domain in achieving PKC isoform selectivity.

Graphical Abstract

*To whom correspondence should be addressed: Tel: 713-743-1708, Fax: 713-743-1884, jdas@uh.edu.

Supporting Information Available

Characterization data for αC1A and αC1B; Emission spectra of curcumin in the presence of varying concentrations of phorbol 13-acetate; Effect of varying concentrations of TPA on the membrane translocation of PKCα and PKCε.

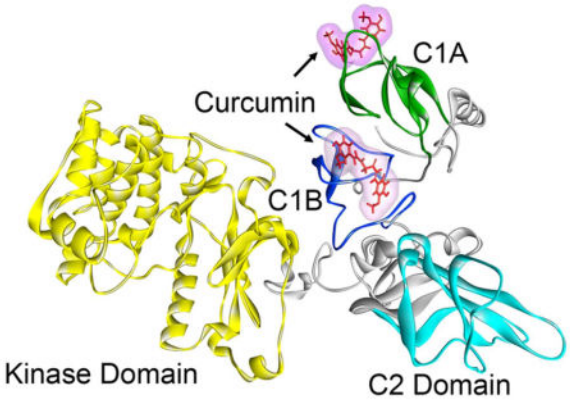

Keywords

Curcumin; polyphenol; protein kinase C; phorbol ester; diacylglycerol; isoform; membrane

Curcumin is a major constituent of turmeric obtained from the powdered root of *Curcuma longa* (1, 2). It is used as a spice to give a specific flavor and yellow color to curry, which is consumed in trace quantities daily by millions of people, particularly from the Asian countries. Curcumin has also been used as a traditional medicine for liver disease (jaundice), indigestion, urinary tract diseases, rheumatoid arthritis, and insect bites (1–3). Research over the last three decades implicated curcumin as a promising therapeutic agent for diseases such as cancer, diabetes, multiple sclerosis, Alzheimer's, HIV and cardiovascular disease (4–6). Curcumin is in the clinical trial for the treatment of colon cancer (7, 8).

Curcumin exerts it pharmacological effect by acting on numerous targets, including protein kinase C (PKC)(9–11). Protein kinase C (PKC) is a family of serine/threonine kinases involved in the regulation of various aspects of cell functions, including cell growth, differentiation, metabolism, and apoptosis(12). Depending on the specificities for Ca^{2+} and the second messenger, diacylglycerol (DAG), the PKC family has been divided into three main groups: conventional isoforms (α, βI, βII and γ) that require Ca^{2+} and DAG for activation; novel isoforms (δ, ε, η, θ and μ) that require only DAG and atypical isoforms (ζ, ι and λ) that require neither Ca^{2+} nor DAG(13). DAG is generated by the phospholipase C-catalyzed hydrolysis of membrane phosphatidylinositol-4,5-bisphosphate (PIP_2). The conventional and novel PKCs have four domains, C1, C2, C3 and C4. The C1 domain consists of a tandem repeat of highly conserved cysteine-rich zinc finger sub-domains, C1A and C1B, which bind DAG/phorbol ester (14). These sub-domains differ in their binding affinities for phorbol ester and DAG. In contrast, the atypical PKCs are non-responsive to DAG/phorbol ester. There is high homology within domains among different members of the superfamily but the novel kinases differ in having the C2 domain at the N-terminal. PKCs are translocated from the cytosol to the plasma membrane, bind to DAG, become activated and subsequently phosphorylate different target proteins (13, 14). Each domain plays a distinct role in the activation and sub-cellular translocation of PKC.

PKC has been implicated in the pathology of several diseases such as cancer, diabetes, stroke, heart failure, and Alzheimer's disease and alcoholism (15–24). PKC has been a subject of intense research and drug development for these disease states for many years and the major challenge has been the selectivity issue- the selectivity not only been within PKC family, but among the 500 kinases. However, in 2012 both FDA and EMA approved a PKC-based drug, ingenol 3-angelate (Picato) for the treatment of actinic keratosis (25–27).

There are multiple studies on the modulation of PKC activity by curcumin (9, 28–36). However, the mechanism by which curcumin modulates PKC activity and the site of its action is poorly understood. Curcumin (< 20 μM) increases the activity of purified PKCα in the presence of membrane(34). At higher curcumin concentrations (> 20 μM), activity is decreased. In another study, it was also shown that curcumin (6–48 μM) activated calcium sensitive PKC (e.g. PKCα) in the presence of membrane and inhibited it in the absence of membrane (33). Similar observation was made in another study in which curcumin (100 μM) inhibited PKC in a membrane-free system (32). All these results indicated that membrane, Ca^{++} and curcumin concentration are important determinants for curcumin's modulation of PKC activity. In cultured NIH3T3 fibroblasts, curcumin (15–20 μM) did not affect the basal PKC activity, but it inhibited the TPA-induced PKC activity (31). In mouse skin, curcumin (10 μmol) inhibited TPA-induced membrane translocation of both PKCα and PKCε (35).

In our previous study we found that curcumin selectively modulated PKCα over PKCε in CHO-K1 cells (36). To understand the mechanism of this selectivity and elucidate the possible role of the PKCα domains responsible for the curcumin binding and modulation, we made several chimeric proteins swapping the C1 and C2 domains of PKCα and PKCε and studied their modulation by curcumin in HEK293 cells. We find that curcumin modulates those proteins where the C1 domain of PKCα is conserved. This result indicates that modulation of PKCα by curcumin is C1 domain dependent.

Material and Methods

General

Curcumin, TPA, phorbol 13-acetate and IPTG were from Sigma. *E. coli* BL21 (DE3) competent cells were obtained from Stratagene, La Jolla, CA, USA. Ni-NTA was from GE Healthcare Life Sciences, Piscataway, NJ, USA. LB (Luria–Bertani) broth medium, TB (terrific broth) medium, and SOC (super optimal culture) were obtained from Invitrogen, Carlsbad, CA, USA. Protein estimations were carried out using the Bradford protein estimation kit from Bio-Rad, Hercules, CA, USA. All the other reagents were from Sigma and of highest purity available.

Construction of Domain Swapped Mutants

The wild type PKCα (αWT) and PKCε (εWT) in pEGFP-N1vector were used to construct six domain swapped mutants by PCR based recombination method. The domain structures of wild type and mutants are shown in Figure 1. Mutants are designed as α/εC2 in which αC2 is replaced with εC2, α/εC1 in which αC1 is replaced with εC1, ε/αC2 in which εC2 is replaced with αC2, ε/αC1 in which εC1 is replaced with αC1, ε/αC1A in which εC1A is

replaced with αC1A and ε/αC1B in which εC1B was replaced with αC1B. Correct sequences in mutants were confirmed by DNA sequencing (SeqWright, Houston, TX).

Cell Culture

The human embryonic kidney 293 (HEK293) cells were cultured in DMEM media supplemented with fetal bovine serum (FBS) and antibiotics (penicillin and streptomycin). Cells were incubated in a humidified atmosphere at 37 °C supplemented with 5% CO_2. HEK293 cells were transfected with wild type and mutant plasmids using Lipofectamine® LTX with Plus™ Reagent (Thermo Fisher Scientific, Grand Island, NY) as per the manufacture's recommendation.

To check the protein expression, transfected cells were lysed in lysis buffer (Cell Signaling, Danvers, MA) and then cell lysates (40–80 μg) were subjected to Western blot analysis. Anti-GFP antibody (1: 1000 dilutions) and anti-β-actin antibody (1: 5000 dilutions) (Cell Signaling, Danvers, MA) were used for protein detection in immunoblots.

Cell Fractionation

Transfected cells were treated with varying concentrations of TPA and curcumin as indicated in the related figures. Cell fractionation and Western blot analysis were carried out as described earlier (36). Briefly, cells were harvested in cell fractionation buffer (20 mM Tris-HCl, pH 7.4) containing phosphates-protein inhibitor (Cell Signaling, Danvers, MA) and lysed by passing the cells through 26 G needle 10 times. Nucleus and unlysed cells were removed by centrifuging at 3500 rpm for 10 min at 4°C. The supernatant was centrifuged at 40,000 rpm for 1 h at 4°C to separate out membrane pellet from the cytosol. This supernatant is the cytosolic extract. The membrane pellet was incubated overnight in cell fractionation buffer containing 1% Triton-X-100 and homogenized by brief sonication. This sonicated solution is the membrane extract. Cytosolic and membrane extracts (20–40 μg) were subjected to SDS-PAGE and immunoblot analysis. The blots were probed with anti-GFP antibody and anti-β-actin antibody. Protein bands were visualized using Enhanced Chemiluminescence Reagent (Thermo Fisher Scientific, Grand Island, NY) and quantified using Alpha Imager Gel Documentation system (Alpha Innotec, Santa Clara, CA).

Confocal Microscopy

Confocal microscopic studies were carried out as described earlier (36). Transfected cells were either treated or co-treated with TPA (10 μM) and curcumin (25 μM) on glass coverslips (VWR, Atlanta, GA) for 1 h. Cells were fixed in 4% paraformaldehyde for 20 min. Coverslips were mounted in anti-fade mounting medium containing DAPI (Vector Laboratories, Inc., Burlingame, CA). Images were collected using Leica SP8 confocal microscope (Leica Microsystems Inc, Buffalo Grove, IL). Sub-cellular distributions of wild type and mutants proteins in confocal images were quantified using ImageJ software (http://rsb.info.nih.gov/ij/)(36).

Protein Purification

The αC1A and αC1B domains in pET28d vector (Novagen, Madison, CA) were used for protein expression (37, 38). The expressed proteins contain a 6-His tag at the N-terminus.

Recombinant plasmids were transformed into BL21 Gold (DE3) cells. The protein expression was induced with IPTG (5 mM) at optical density (OD) of 0.7 and then cells were allowed to grow for overnight at 18°C. Cells expressing αC1A and αC1B were re-suspended in lysis buffer A (50 mM Tris-HCl, pH 8.0, 150 mM NaCl, 50 mM urea, 10 mM imidazole) and lysis buffer B (50 mM Tris-HCl, pH 8.0, 150 mM NaCl, 10 mM imidazole), respectively. Cells were lysed by sonication (2 min, 30% amplitude, 3s on and 3s off cycle) and soluble proteins were obtained by centrifugation at 15,000g for 15 min at 4 °C. Extracted lysates were incubated with Ni-NTA bound agarose beads for 1 h and then washed with respective lysis buffer to remove unbound proteins. Bound proteins were eluted in lysis buffer containing 300 mM imidazole. Eluted protein fractions were pooled, concentrated and further purified on size exclusion column (Sephadex 75 10/300 GL, GE Life Science, Madison, CA) using gel filtration buffer (50 mM Tris-HCl, pH 8.0, 300 mM NaCl). Purity of the proteins was determined by SDS-PAGE (15%) and Coomassie blue staining.

Fluorescence Measurements

Fluorescence measurements were carried out using PTI LPS 220B fluorimeter equipped with temperature and stirring control systems (Photon Technology Instruments, Princeton, NJ). For intrinsic fluorescence measurements, proteins (1 μM) in buffer (50 mM Tris, 150 mM NaCl, pH 7. 2) were excited at 290 nm and emission spectra were recorded from 300 nm to 500 nm. For binding assay, emission spectra of curcumin (5 μM) were measured in the presence of varying concentration of protein (1–5 μM) and TPA (1–10 μM). Sample mixtures in buffer (50 mM Tris, 150 mM NaCl, pH 7.2) were incubated for 30 min at room temperature before each measurement. Curcumin was excited at 425 nm and emission spectra were recorded from 440 nm to 700 nm. Maximum (Em_{max}) of the emission spectrum was determined by a Gaussian function fit using IGOR Pro (WaveMatrix, Lake Oswego, OR). The change in fluorescence intensity at Em_{max} for each concentration of TPA was normalized using the equation: $(F_i - F_0)/F_0$, where F_i and F_0 are fluorescence intensities of curcumin with and without TPA. IC_{50} was measured from the fitted curve using Hill equation in Sigma Plot 11 (Systat Software Inc., San Jose, CA).

Structure Prediction and Validation

PKCα (Uniprot: P17252) protein sequence was used to predict the 3D structure using Robetta protein structure prediction server (http://robetta.bakerlab.org) (39, 40). This server predicts the model based on available structure and *ab initio* prediction methods. Homology models of C1A, C1B, C2 and kinase domain of PKCα were generated using templates having PDB codes 2E73, 2ELI, 3GPE and 3IW4, respectively. Overall quality factor such as, covalent bond distances, bond angles, stereo chemical validation, atom nomenclature and non-bonded interactions between different atoms types were validated using SAVS server.

Molecular Docking

Curcumin was docked into PKCαC1A and PKCαC1B domains using Sybyl X 2.1. The model of PKCα (described in the previous section) was used for the protein structure, and curcumin structure was generated using ChemBioDraw 12.0. For the docking simulation, protomols were created by Sybyl for a docking space of ligand by selecting the specific residues within radius of 3Å. The ligand binding pocket was defined between the two loops

of a C1 domain using the homologous phorbol ester binding residues of PKCδC1B (41, 42). Threshold 0.5 and Bloat 4.0 were used to create the protomols. After generating the protomol, the docking simulations were performed using Surflexdock Geom module of Sybyl.

Molecular Dynamics Simulation

Molecular dynamics (MD) simulations were performed on the four simulating systems consisting of free PKCα, PKCα with curcumin on C1A, PKCα with curcumin on C1B, and PKCα with curcumin on both C1A and C1B. For the MD simulation, the conformation that showed the highest docking score was selected. The MD simulations were carried out using the GROMACS 4.6.5 package of programs (43) with Amber99sb force field (44). The topology and coordinate files of curcumin (CUR) were generated by Antechamber program in AMBER tool were converted to GROMACS format using ACPYPE (45). The models were solvated by TIP3P water molecules (46) with a box distance of 1.0 nm and neutralized by adding four Na^+ counter ions. For the free protein, 48,973 water molecules were used to solvate the system. Energy minimization was completed using the steepest descent method for 5000 steps to remove steric clashes generated while solvating the system. After energy minimization, the minimized systems were equilibrated for 200 ps by position restrained MD simulation in order to maintain temperature and pressure of systems and relax the solvent. The equilibration was performed in two phases. NVT optimization with 300 K was conducted in the first phase, and the second phase was conducted for NPT optimization with 1 bar. Following the equilibration, MD production run was carried out using the Berendsen coupling method (47) with 300 K and 1 bar for 1.0 ns in all systems. The bond lengths were constrained by LINCS algorithm (48) allowing a time step of 2 fs. The Particle Mesh Ewald (PME) method (49) was used to compute electrostatic interactions. The van der Waals, electrostatic, and coulombic interactions were calculated with a 1 nm cut-off. For analysis, the atomic coordinates were saved every 10 ps during the MD simulation.

The MD trajectories of the four systems were analyzed by GROMACS analysis tools, including g_energy and g_rms. The graphs were plotted by QtGrace. The trajectories and structures were visualized using PyMol v1.7 (Schrodinger, LLC) and Discovery Studio Visualizer 4.5 (Biovia Inc.)

Statistical Analysis

Statistical analyses were performed using Sigma Plot 11. All the statistical analyses in figures were based on three independent experiments. The results were expressed as the mean ± SEM. Statistical significance was established by one-way ANOVA, followed by Bonferroni *post hoc* test. A value of $P < 0.05$ was considered significant.

Results

Generation of domain-swapped mutants of PKCα and PKCε

We have recently shown that curcumin inhibits TPA-induced membrane translocation of PKCα, but not PKCε in CHO-K1 cells (36). PKCα (αWT) and PKCε (εWT) differ in the position of their C1 and C2 domain structure, as shown in figure 1. C1 and C2 domains of

PKCα and PKCε show differences in their ligand/cofactor binding properties. C1 domain of PKCα and PKCε is composed of C1A and C1B sub-domains and binds to DAG/TPA, but their affinity varies within the sub-domain. C2 domain of PKCα, but not PKCε binds to Ca^{++}. To investigate if structural differences in PKCα and PKCε are responsible for curcumin inhibition, we made six C1 and C2 domain-swapped mutants of PKCα (α/εC2, α/εC1) and PKCε (ε/αC1, ε/αC2, ε/αC1Aε, ε/αC1B) (Fig. 1) and studied their TPA-induced membrane translocation in transiently transfected HEK293 cells in the presence and absence of curcumin.

Expression of the mutants in HEK293 cells

To examine the effect of domain swapping on the level of protein expression, whole cell lysates of αWT, εWT and their mutants prepared from the same amounts of cells were analyzed by immuno-blot analysis (Fig. 2). Expression level of εWT was 2-fold higher as compared to αWT. However, expression of α/εC1, α/εC2, ε/αC1, ε/αC2, ε/αC1A, and ε/αC1B was significantly lower as compared to the wild type (αWT and εWT). C2 domain swapped mutants (α/εC2 and ε/αC2) showed reduced (~50%) protein expression as compared to C1 domain-swapped mutants (α/εC1 and ε/αC1). The expression level of ε/αC1A and ε/αC1B are similar to that of ε/αC1 mutant. In conclusion, C1 and C2 domain swapping in PKCα and PKCε affected protein expression in HEK 293 cells, but the level of expression of all the mutants are adequate for the membrane translocation assays.

Effect of curcumin on domain swapped mutants of PKCα and PKCε in HEK293 cells

To study the effect of curcumin on mutant proteins, we measured their TPA-induced membrane translocation from cytosol to membrane in the presence and the absence of curcumin (Fig. 3). Treatment with curcumin (25 μM) alone did not show any effect on the distribution of wild type and mutant proteins in cytosol and membrane, as protein levels were similar in cytosol and membrane for curcumin-treated and control cells. However, αWT and εWT translocated from cytosol to membrane upon treatment with as low as 100 nM TPA, as we detected most of the proteins in the membrane. This result is consistent with our earlier report in CHO-K1 cells (36). Likewise, mutants α/εC1 and ε/αC1 were also translocated to the membrane upon TPA treatment, but at much higher concentration as compared to the wild type proteins. At 10 μM, majority of the protein is translocated to the membrane. In contrast, mutants α/εC2 and ε/αC2 did not show TPA-induced membrane translocation even at a TPA concentration of 10 μM. Therefore, we decided to compare TPA-induced membrane translocation studies of αWT, εWT, α/εC1 and ε/αC1 at 10 μM TPA for studying the effect of curcumin on their TPA-induced membrane translocation. This concentration of TPA was used by several PKC research groups earlier (50–52). Moreover, we did not observe any hyper-activation dependent degradation of αWT and εWT at this dose (Fig. S1). When curcumin was co-treated with TPA, the level of αWT in the membrane was significantly reduced (~ 50%) as compared with cells treated with TPA alone. For εWT, however, the protein level in the membrane was similar for cells either with TPA or TPA plus curcumin co-treatment. In contrast, co-treatment of TPA and curcumin significantly reduced (~40%) the TPA-induced membrane translocation of ε/αC1, when compared with cells treated with TPA alone. On the other hand, α/εC1 did not show any reduction in the TPA-induced membrane translocation when co-treated with TPA and curcumin.

Furthermore, TPA and curcumin co-treatment did not have any effect on α/εC2 and ε/αC2 mutants as the protein level in cytosol and membrane were similar to control cells. In summary, these results indicate that αC1 domain is responsible for curcumin's inhibitory effects on TPA-induced membrane translocation of PKCα and C2 domain-swapped mutants are not sensitive to TPA or TPA plus curcumin co-treatment.

Effect of curcumin on TPA-induced membrane translocation of ε/αC1A and ε/αC1B mutants

C1 domain of PKC is comprised of C1A and C1B sub-domains. To pin point the site of action of curcumin in αC1 domain and to understand the role of αC1A and αC1B sub-domains, we constructed ε/αC1A and ε/αC1B mutants, where C1A and C1B of PKCε was replaced with C1A and C1B of PKCα, respectively and studied their translocation in response to curcumin and TPA using confocal microscopy as described in the previous section (Fig. 4A). Curcumin treatment did not show any effect on ε/αC1A and ε/αC1B as most of the protein were localized to cytosol like control cells. But, ε/αC1A and ε/αC1B mutant proteins were localized to membrane in TPA-treated cells. However, cells co-treated with curcumin and TPA showed significant reduction (30–40%) in the amounts of ε/αC1A and ε/αC1B in the membrane, when compared with TPA treated cells. These results were further confirmed by cell fractionation and immunoblot analysis (Fig. 4B). In this experiment, cells were treated with varying concentration of TPA (0–10 μM) and also co-treated with curcumin (25 μM) and TPA for 1 h. Amounts of ε/αC1A and ε/αC1B in cytosol were measured. TPA treatment decreased the cytosolic ε/αC1A and ε/αC1B in a dose-dependent manner. However, amounts of ε/αC1A and ε/αC1B in cytosol were significantly higher in co-treated cells compared to the TPA-treated cells. Thus, using both confocal microscopy and Western blot analysis we conclude that both αC1A and αC1B sub-domains are involved in inhibitory effects of curcumin.

Effect of phorbol 13-acetate on curcumin binding to αC1A and αC1B

To determine, if observed inhibition of PKCα by curcumin is due to its competition with TPA binding site in αC1A and αC1B, we examined its binding to αC1A and αC1B using *in vitro* fluorescence assay. For this, the isolated αC1A and αC1B sub-domains were expressed in *E. coli* and then purified by 6His-affinity chromatography. Purified proteins were thoroughly characterized by SDS-PAGE and tryptophan fluorescence studies (Fig. S2). αC1A, which contains a tryptophan residue in its primary sequence, showed tryptophan fluorescence with an emission maximum at 335 nm. αC1B, on the other hand, does not have tryptophan residue in its primary sequence and show very weak fluorescence (Fig. S2B). For the binding studies, fluorescence of curcumin was measured in the absence and the presence of protein and/or phorbol 13-acetate. Significantly higher fluorescence intensity with prominent blue shift of the emission maximum of curcumin was observed in the presence of proteins indicating curcumin's binding to protein (Fig. 5A). The observed blue shift was from 577 nm (in buffer) to 552 nm and 565 nm in the presence of αC1B and αC1A, respectively. Moreover, the decrease in curcumin-protein fluorescence intensity with increasing concentration of phorbol 13-acetate indicated that curcumin is competitively displaced from the phorbol ester site of αC1B and αC1A (Fig. 5B). Fitting these fluorescence data with Hill's equation results in the IC_{50} values of 4.47±1.7 μM and

6.27±1.2 μM for αC1B and αC1A, respectively, indicating that the site of action of curcumin is the phorbol ester binding site in αC1B and αC1A, and C1B has higher binding affinity than C1A.

Molecular docking and molecular dynamics simulation

To understand the site of curcumin action in PKCα from a structural viewpoint, curcumin was docked into C1A and C1B of full-length PKCα structure. The simple homology model of PKCα using PKC®II (PDB code: 3PFQ) as the template could not be generated because several regions of PKC®II were unresolved in the structure. We therefore used a server-based automated program Robetta to generate the PKCα structure. To understand the modes of curcumin binding, we docked curcumin into the both to the C1A and C1B sub-domains, and then MD simulations were performed for four systems-free PKCα, PKCα with curcumin on C1A, PKCα with curcumin on C1B, and PKCα with curcumin on both C1A and C1B during 1.0 ns. The docking results revealed that curcumin formed two hydrogen bonds with C1A residues while it formed 10 hydrogen bonds with the binding cleft residues in C1B, resulting in the docking score of 5.0 and 5.14 for C1A and C1B respectively. Using these Surflex-Dock score the estimated K_d values for the C1A and C1B are calculated to be 8.523 μM and 7.56 μM, respectively (53).

The potential energy plot showed that the four molecular systems were quickly stabilized and remained stable during 1.0 ns MD simulation (Fig. 6). The potential energies were similar with or without curcumin docking and independent of the type of C1 domain. The ligand-free PKCα and PKCα with curcumin on C1B changed their conformation most at 400 ps, but the RMSD values of PKCα with curcumin on C1A and PKCα with curcumin on both C1A and C1B steadily increased after 400 ps (Fig. 6A). At 1 ns, however, PKCα with curcumin docked on C1B showed the lowest RMSD compared to the other three structures. The variation of RMSD values for the three structures are shown in figure 6B.

Discussion

Our recent observation is that curcumin selectively inhibits PKCα over PKCε in CHO-K1 cells (36). As a follow up study, here we sought to pinpoint the domain of PKCα responsible for binding to curcumin and inhibiting its phorbol ester-induced membrane translocation. To do so, we have generated several chimeric proteins by swapping the C1 and C2 domains of PKCα and PKCε. C1 domain, which consists of C1A and C1B sub-domains, shows differential phorbol ester/DAG binding affinity and play divergent roles for the membrane translocation and activation of these two PKC isoforms (37, 54). Similarly, C2 domains of these two isoforms show very distinct properties: C2 domain of PKCα binds to Ca^{++}, but C2 of PKCε does not. The kinase domains (C3 and C4) of PKCα and PKCε are highly conserved both structurally and functionally. While our previous study was done with CHO-K1 cells in which PKCα and PKCε were expressed endogenously, in the present study we used the EGFP-tagged chimeric proteins heterologously expressed in HEK293 cells. All the mutants are expressed in HEK293 cells in adequate amounts for measuring the membrane translocation using confocal microscopy. Like in CHO-K1 cells, curcumin also selectively inhibited phorbol ester-induced membrane translocation of PKCα, but not PKCε in HEK293

cells (Fig. 3) demonstrating that both cell lines are compatible for studying PKC-curcumin interactions.

In its activation mechanism, PKCα initially binds to the surface of the membrane through a low affinity interaction between the Ca^{++} -binding sites of the C2 domain and the head groups of anionic lipid, phosphatidylserine present in the plasma membrane. The C1 domains then insert into the membrane-interior with higher affinity by binding with DAG or phorbol ester (14). The crystal structure of phorbol 13-acetate bound C1B reveals that binding of phorbol ester to the C1 domain caps the hydrophilic base of the phorbol-binding site to form a contiguous hydrophobic surface thereby increasing the affinity of the phorbol-C1 complex for the membrane (41). The combined interaction of the C1 and C2 domains with the membrane forms a milieu that provides the energy for the optimal conformational change for activation, which results in the release of the pseudosubstrate domain from the active site of the enzyme. The observed inhibitory effects of curcumin on PKCα activity could result from its interference on the association of PKCα with membranes by binding to the either C2 domain or C1 domain. Our result that curcumin inhibits phorbol ester-induced membrane translocation of PKCε mutants, in which εC1 domain is replaced with αC1, but not the PKCα mutants in which αC1 is replaced with εC1 domain, suggests that αC1 is a determinant for curcumin's effect. Having identified the C1 domain of PKCα as the primary site of curcumin's action, we further asked if C1A and/or C1B are important for such action. To address this we made two additional mutants of PKCε in which εC1A and εC1B were replaced by αC1A and αC1B, respectively. We found that curcumin inhibited membrane translocation of both these PKCε mutants indicating curcumin's affinity for both αC1A and αC1B domains. To further determine the relative affinity of curcumin for the αC1A and αC1B sub-domains, we studied their interactions with curcumin using a fluorescence assay previously used to study the effect of resveratrol with PKC (55). Resveratrol is another naturally occurring polyphenol known for its interaction with PKC (56). Our results show that phorbol 13-acetate displaced curcumin from αC1A and αC1B with IC_{50} values of 6.27± 1.2 μM and 4.47±1.7 μM, respectively, indicating slightly higher affinity of the αC1B than αC1A. This is also in agreement with the docking score obtained from the molecular docking of curcumin into the phorbol ester binding site of C1A and C1B of PKCα (Fig. 7). Whereas curcumin forms two hydrogen bonds with αC1A, it forms 10 hydrogen bonds with αC1B, with docking score of 5.0 and 5.14 for C1A and C1B, respectively, showing higher affinity for C1B than C1A. Further, molecular dynamics (MD) simulation (1 ns) studies indicated that the potential energy and backbone flexibility (reflected by the RMSD values) for three structures, curcumin docked into C1A, curcumin docked into C1B and curcumin docked into both C1A and C1B were similar at 1 ns (Fig. 6A), again indicating that curcumin can act on both C1A and C1B.

Our *in vitro* binding results suggest that phorbol ester has higher affinity than curcumin in the absence of membrane lipids. Of course, the affinities could vary in the presence of lipids. However because of its lower affinity curcumin does not completely inhibit phorbol ester-induced translocation. We see ~46% inhibition at 25 μM curcumin (Fig. 3).

Does the C1 domain confer curcumin's selectivity for PKCα over PKCε? The C1 domains are highly conserved in their sequence and overall structure (14, 42), *a priori*. Comparison of

the αC1A and αC1B reveals 67% and 62% sequence identity with εC1A and εC1B, respectively. It is possible that the structural differences between the αC1 and εC1 could lead to their different affinity for curcumin. However, unavailability of the structures of the αC1A, εC1A and εC1B does not allow us to compare directly the structure and the side chain orientation of the residues in the ligand binding site of PKCα and PKCε C1 domains. Our recent observation of the distinctly different orientation of the homologous Trp-22 in PKCθC1B (57), Munc13 C1 (58) and PKCδC1B (41) led us to believe that such subtle differences may exist in the curcumin binding site of C1 domains of PKCα and PKCε. Based on the δC1B-phorbol 13-acetate crystal structure (41), residues in the phorbol ester binding side in PKCα and PKCε show sequence identity of 66.6% for C1A and 75% for C1B (Fig 8). In the phorbol ester binding domain, Phe-8, Lys-9, Phe-13 and Phe-24 in αC1A are replaced by Leu-8, Arg-9, Tyr-13 and Val-24, respectively in εC1A. Among these, Phe-24 and Val-24 are located at the tip of the loop and interact with the membrane directly. Similarly, for the phorbol ester binding domain of C1B, Gly-9, Ser-10 and Tyr-22 in αC1B are replaced by Lys-9, Val-10 and Trp-22, respectively in εC1B. Among these, Tyr/Trp switch at position 22 is known to modulate the membrane affinity for conventional and novel PKC (59). Moreover, whereas PKCα shows high selectivity for PS (60), PKCε shows little selectivity for it (54). Also, that curcumin is also known to alter the structure and properties of lipid bilayer (61–63), it is highly likely that the affinity of PKCα, PKCε or their complex with curcumin for plasma membrane would vary.

The inability of the C2 domain swapped mutants, α/εC2 and ε/αC2 to respond to TPA-induced membrane translocation did not allow us to study the role of C2 domain on curcumin's inhibitory effects of TPA-induced membrane translocation. This also demonstrates that C2 domain is critical for PKC functionality. This calcium-binding domain also binds to the isoform-specific RACK proteins which aid to the membrane translocation of PKC (64, 65). In a recent study on the effects of curcumin on PKCα using purified protein, Perez-Lara et al. showed that PKC modulation, in fact, was dependent on the presence and absence of a membrane rather than the calcium concentration (34), ruling out the calcium-binding C2 domain's involvement in the modulation by curcumin. However, this cannot completely preclude the role of C2 domain since ours is a membrane translocation assay in a cellular environment and their assay was done using purified protein. It is possible that C2 domain could influence the binding of C1 domain to the membrane since there are several residues of C2 domain that interact with the C1 domain (66). Further studies are required to clarify the role of C2 domain in this process.

In summary, our results show that curcumin inhibits PKCα by binding to its C1 domain. This study highlights the importance of targeting C1 domains in developing isoform selective molecules for drug development. PKCα is an important regulator of cardiovascular function, platelet function and cancer (67, 68). Now that the site of action of is known, curcumin or its high affinity analogs with improved pharmacokinetic properties can be designed for treating the related disease states.

Supplementary Material

Refer to Web version on PubMed Central for supplementary material.

Acknowledgments

MD simulations were performed using the server at the High Performance Computing Center of University of Houston.

Funding Information This research has been supported by funding from NIH grant 1R01 AA022414-01A1 to Joydip Das.

Abbreviations

PKC	protein kinase C
DAG	diacylglycerol
TPA	12-O-tetradecanoylphorbol-13-acetate
PS	phosphatidylserine
FBS	fetal bovine serum
DMSO	dimethyl sulfoxide
SDS-PAGE	sodium dodecyl sulfonate- polyacrylamide gel electrophoresis
FITC	fluorescein isothiocyanate
FDA	food and drug administration
EMA	European medicines agency
HEK	human embryonic kidney
CHO	Chinese hamster ovary
IPTG	isopropyl β-D-1-thiogalactopyranoside
EGFP	enhanced green fluorescent protein
Ni-NTA	nickel nitrilotriacetic acid

References

1. Goel A, Aggarwal BB. Curcumin, the golden spice from Indian saffron, is a chemosensitizer and radiosensitizer for tumors and chemoprotector and radioprotector for normal organs. Nutr Cancer. 2010; 62:919–930. [PubMed: 20924967]
2. Epstein J, Sanderson IR, Macdonald TT. Curcumin as a therapeutic agent: the evidence from in vitro, animal and human studies. Br J Nutr. 2010; 103:1545–1557. [PubMed: 20100380]
3. Singh S. From exotic spice to modern drug? Cell. 2007; 130:765–768. [PubMed: 17803897]
4. Ataie A, Sabetkasaei M, Haghparast A, Moghaddam AH, Ataee R, Moghaddam SN. Curcumin exerts neuroprotective effects against homocysteine intracerebroventricular injection-induced cognitive impairment and oxidative stress in rat brain. J Med Food. 2010; 13:821–826. [PubMed: 20553189]
5. Cemil B, Topuz K, Demircan MN, Kurt G, Tun K, Kutlay M, Ipcioglu O, Kucukodaci Z. Curcumin improves early functional results after experimental spinal cord injury. Acta Neurochir (Wien). 2010; 152:1583–1590. discussion 1590. [PubMed: 20535508]

6. Morimoto T, Sunagawa Y, Fujita M, Hasegawa K. Novel heart failure therapy targeting transcriptional pathway in cardiomyocytes by a natural compound, curcumin. Circ J. 2010; 74:1059–1066. [PubMed: 20467147]
7. Gupta SC, Patchva S, Aggarwal BB. Therapeutic roles of curcumin: lessons learned from clinical trials. AAPS J. 2013; 15:195–218. [PubMed: 23143785]
8. Carroll RE, Benya RV, Turgeon DK, Vareed S, Neuman M, Rodriguez L, Kakarala M, Carpenter PM, McLaren C, Meyskens FL Jr, Brenner DE. Phase IIa clinical trial of curcumin for the prevention of colorectal neoplasia. Cancer Prev Res (Phila). 2011; 4:354–364. [PubMed: 21372035]
9. Lin JK. Molecular targets of curcumin. Adv Exp Med Biol. 2007; 595:227–243. [PubMed: 17569214]
10. Zhou H, Beevers CS, Huang S. The targets of curcumin. Curr Drug Targets. 2011; 12:332–347. [PubMed: 20955148]
11. Gupta SC, Prasad S, Kim JH, Patchva S, Webb LJ, Priyadarsini IK, Aggarwal BB. Multitargeting by curcumin as revealed by molecular interaction studies. Nat Prod Rep. 2011; 28:1937–1955. [PubMed: 21979811]
12. Battaini F, Mochly-Rosen D. Happy birthday protein kinase C: past, present and future of a superfamily. Pharmacol Res. 2007; 55:461–466. [PubMed: 17582783]
13. Newton AC. Protein kinase C: structural and spatial regulation by phosphorylation, cofactors, and macromolecular interactions. Chem Rev. 2001; 101:2353–2364. [PubMed: 11749377]
14. Das J, Rahman GM. C1 domains: structure and ligand-binding properties. Chem Rev. 2014; 114:12108–12131. [PubMed: 25375355]
15. Hofmann J. Protein kinase C isozymes as potential targets for anticancer therapy. Curr Cancer Drug Targets. 2004; 4:125–146. [PubMed: 15032665]
16. Mochly-Rosen D, Das K, Grimes KV. Protein kinase C, an elusive therapeutic target? Nat Rev Drug Discov. 2012; 11:937–957. [PubMed: 23197040]
17. Koivunen J, Aaltonen V, Peltonen J. Protein kinase C (PKC) family in cancer progression. Cancer Lett. 2006; 235:1–10. [PubMed: 15907369]
18. Griner EM, Kazanietz MG. Protein kinase C and other diacylglycerol effectors in cancer. Nat Rev Cancer. 2007; 7:281–294. [PubMed: 17384583]
19. Das Evcimen N, King GL. The role of protein kinase C activation and the vascular complications of diabetes. Pharmacol Res. 2007; 55:498–510. [PubMed: 17574431]
20. Bright R, Mochly-Rosen D. The role of protein kinase C in cerebral ischemic and reperfusion injury. Stroke. 2005; 36:2781–2790. [PubMed: 16254221]
21. Chou WH, Messing RO. Protein kinase C isozymes in stroke. Trends Cardiovasc Med. 2005; 15:47–51. [PubMed: 15885569]
22. Sabri A, Steinberg SF. Protein kinase C isoform-selective signals that lead to cardiac hypertrophy and the progression of heart failure. Mol Cell Biochem. 2003; 251:97–101. [PubMed: 14575310]
23. Alkon DL, Sun MK, Nelson TJ. PKC signaling deficits: a mechanistic hypothesis for the origins of Alzheimer's disease. Trends Pharmacol Sci. 2007; 28:51–60. [PubMed: 17218018]
24. Pany S, Das J. Alcohol binding in the C1 (C1A+C1B) domain of protein kinase C epsilon. Biochim Biophys Acta. 2015; 1850:2368–2376. [PubMed: 26210390]
25. Lebwohl M, Swanson N, Anderson LL, Melgaard A, Xu Z, Berman B. Ingenol mebutate gel for actinic keratosis. New Eng J Med. 2012; 366:1010–1019. [PubMed: 22417254]
26. Kedei N, Lundberg DJ, Toth A, Welburn P, Garfield SH, Blumberg PM. Characterization of the interaction of ingenol 3-angelate with protein kinase C. Cancer Res. 2004; 64:3243–3255. [PubMed: 15126366]
27. Ogbourne SM, Hampson P, Lord JM, Parsons P, De Witte PA, Suhrbier A. Proceedings of the First International Conference on PEP005. Anti-cancer Drugs. 2007; 18:357–362. [PubMed: 17264770]
28. Lin JK, Chen YC, Huang YT, Lin-Shiau SY. Suppression of protein kinase C and nuclear oncogene expression as possible molecular mechanisms of cancer chemoprevention by apigenin and curcumin. J Cell Biochem Suppl. 1997; 28–29:39–48.
29. Rungseesantivanon S, Thenchaisri N, Ruangvejvorachai P, Patumraj S. Curcumin supplementation could improve diabetes-induced endothelial dysfunction associated with decreased vascular

superoxide production and PKC inhibition. BMC Complement Altern Med. 2010; 10:57. [PubMed: 20946622]

30. Balasubramanyam M, Koteswari AA, Kumar RS, Monickaraj SF, Maheswari JU, Mohan V. Curcumin-induced inhibition of cellular reactive oxygen species generation: novel therapeutic implications. J Biosci. 2003; 28:715–721. [PubMed: 14660871]
31. Liu JY, Lin SJ, Lin JK. Inhibitory effects of curcumin on protein kinase C activity induced by 12-O-tetradecanoyl-phorbol-13-acetate in NIH 3T3 cells. Carcinogenesis. 1993; 14:857–861. [PubMed: 8504477]
32. Reddy S, Aggarwal BB. Curcumin is a non-competitive and selective inhibitor of phosphorylase kinase. FEBS Lett. 1994; 341:19–22. [PubMed: 7511111]
33. Mahmmoud YA. Modulation of protein kinase C by curcumin; inhibition and activation switched by calcium ions. Br J Pharmacol. 2007; 150:200–208. [PubMed: 17160011]
34. Perez-Lara A, Corbalan-Garcia S, Gomez-Fernandez JC. Curcumin modulates PKCalpha activity by a membrane-dependent effect. Arch Biochem Biophys. 2011; 513:36–41. [PubMed: 21741352]
35. Garg R, Ramchandani AG, Maru GB. Curcumin decreases 12-O-tetradecanoylphorbol- 13-acetate-induced protein kinase C translocation to modulate downstream targets in mouse skin. Carcinogenesis. 2008; 29:1249–1257. [PubMed: 18477648]
36. Pany S, Majhi A, Das J. Selective Modulation of Protein Kinase C alpha over Protein Kinase C epsilon by Curcumin and Its Derivatives in CHO-K1 Cells. Biochemistry. 2016; 55:2135–2143. [PubMed: 26983836]
37. Ananthanarayanan B, Stahelin RV, Digman MA, Cho W. Activation mechanisms of conventional protein kinase C isoforms are determined by the ligand affinity and conformational flexibility of their C1 domains. J Biol Chem. 2003; 278:46886–46894. [PubMed: 12954613]
38. Cho W, Digman M, Ananthanarayanan B, Stahelin RV. Bacterial expression and purification of C1 and C2 domains of protein kinase C isoforms. Methods Mol Biol. 2003; 233:291–298. [PubMed: 12840516]
39. Kim DE, Chivian D, Baker D. Protein structure prediction and analysis using the Robetta server. Nucleic Acids Res. 2004; 32:W526–531. [PubMed: 15215442]
40. Celic A, Petri ET, Demeler B, Ehrlich BE, Boggon TJ. Domain mapping of the polycystin-2 C-terminal tail using de novo molecular modeling and biophysical analysis. J Biol Chem. 2008; 283:28305–28312. [PubMed: 18694932]
41. Zhang G, Kazanietz MG, Blumberg PM, Hurley JH. Crystal structure of the cys2 activator-binding domain of protein kinase C delta in complex with phorbol ester. Cell. 1995; 81:917–924. [PubMed: 7781068]
42. Rahman GM, Das J. Modeling studies on the structural determinants for the DAG/phorbol ester binding to C1 domain. J Biomol Struct Dyn. 2015; 33:219–232. [PubMed: 24666138]
43. Hess B, Kutzner C, van Der Spoel D, Lindahl E. GROMACS 4: Algorithms for Highly Efficient, Load-Balanced, and Scalable Molecular Simulation. J Chem Ther Comput. 2008; 4:435–447.
44. Viktor H, Abel R, Okur A, Strockbine B, Roitberg A, Simmerling C. Comparison of multiple Amber force fields and development of improved protein backbone parameters. Proteins: Structure, Function, and Bioinformatics. 2006; 65:712–725.
45. WSdSAFVW. ACPYPE - AnteChamber PYthon Parser interfacE. BMC Res Notes. 2012; 5:367. [PubMed: 22824207]
46. Jorgensen WL, Chandrasekhar J, Madura JD, Impey RW, Klein ML. Comparison of simple potential functions for simulating liquid water. J Chem Phys. 1983; 79:926–935.
47. Berendsen HJ, van Postma JPM, van Gunsteren Wilfred F, DiNola ARHJ, Haak JR. Molecular dynamics with coupling to an external bath. J Chem Phys. 1984; 81:3684–3690.
48. Hess B, Bekker H, Berendsen HJC, Fraaije JGEM. LINCS: A linear constraint solver for molecular simulations. J Comput Chem. 1997; 18:1463–1472.
49. Essmann U, Perera L, Berkowitz ML, Darden T, Lee H, Pedersen LG. A smooth particle mesh Ewald method. J Chem Phys. 1995; 103:8577–8593.
50. Slater SJ, Kelly MB, Larkin JD, Ho C, Mazurek A, Taddeo FJ, Yeager MD, Stubbs CD. Interaction of alcohols and anesthetics with protein kinase Cα. J Biol Chem. 1997; 272:6167–6173. [PubMed: 9045629]

51. Giorgione J, Hysell M, Harvey DF, Newton AC. Contribution of the C1A and C1B domains to the membrane interaction of protein kinase C. Biochemistry. 2003; 42:11194–11202. [PubMed: 14503869]
52. Geczy T, Peach ML, El Kazzouli S, Sigano DM, Kang JH, Valle CJ, Selezneva J, Woo W, Kedei N, Lewin NE. Molecular basis for failure of “atypical” C1 domain of Vav1 to bind diacylglycerol/phorbol ester. J Biol Chem. 2012; 287:13137–13158. [PubMed: 22351766]
53. Jain AN. Scoring noncovalent protein-ligand interactions: a continuous differentiable function tuned to compute binding affinities. J Comput Aided Mol Des. 1996; 10:427–440. [PubMed: 8951652]
54. Stahelin RV, Digman MA, Medkova M, Ananthanarayanan B, Melowic HR, Rafter JD, Cho W. Diacylglycerol-induced membrane targeting and activation of protein kinase Cepsilon: mechanistic differences between protein kinases Cdelta and Cepsilon. J Biol Chem. 2005; 280:19784–19793. [PubMed: 15769752]
55. Slater SJ, Seiz JL, Cook AC, Stagliano BA, Buzas CJ. Inhibition of protein kinase C by resveratrol. Biochim Biophys Acta. 2003; 1637:59–69. [PubMed: 12527408]
56. Das J, Ramani R, Suraju MO. Polyphenol compounds and PKC signaling. Biochim Biophys Acta. 2016; 1860:2107–2121. [PubMed: 27369735]
57. Rahman GM, Shanker S, Lewin NE, Kedei N, Hill CS, Prasad BV, Blumberg PM, Das J. Identification of the activator-binding residues in the second cysteine-rich regulatory domain of protein kinase Ctheta (PKCtheta). Biochem J. 2013; 451:33–44. [PubMed: 23289588]
58. Shen N, Guryev O, Rizo J. Intramolecular occlusion of the diacylglycerol-binding site in the C1 domain of munc13-1. Biochemistry. 2005; 44:1089–1096. [PubMed: 15667202]
59. Dries DR, Gallegos LL, Newton AC. A single residue in the C1 domain sensitizes novel protein kinase C isoforms to cellular diacylglycerol production. J Biol Chem. 2007; 282:826–830. [PubMed: 17071619]
60. Medkova M, Cho W. Differential membrane-binding and activation mechanisms of protein kinase C-alpha and -epsilon. Biochemistry. 1998; 37:4892–4900. [PubMed: 9538007]
61. Hung WC, Chen FY, Lee CC, Sun Y, Lee MT, Huang HW. Membrane-thinning effect of curcumin. Biophys J. 2008; 94:4331–4338. [PubMed: 18310254]
62. Barry J, Fritz M, Brender JR, Smith PE, Lee DK, Ramamoorthy A. Determining the effects of lipophilic drugs on membrane structure by solid-state NMR spectroscopy: the case of the antioxidant curcumin. J Am Chem Soc. 2009; 131:4490–4498. [PubMed: 19256547]
63. Perez-Lara A, Ausili A, Aranda FJ, de Godos A, Torrecillas A, Corbalan-Garcia S, Gomez-Fernandez JC. Curcumin disorders 1,2-dipalmitoyl-sn-glycero-3-phosphocholine membranes and favors the formation of nonlamellar structures by 1,2-dielaidoyl-sn-glycero-3-phosphoethanolamine. J Phys Chem B. 2010; 114:9778–9786. [PubMed: 20666521]
64. Ron D, Luo J, Mochly-Rosen D. C2 region-derived peptides inhibit translocation and function of beta protein kinase C in vivo. J Biol Chem. 1995; 270:24180–24187. [PubMed: 7592622]
65. Banci L, Cavallaro G, Kheifets V, Mochly-Rosen D. Molecular dynamics characterization of the C2 domain of protein kinase Cbeta. J Biol Chem. 2002; 277:12988–12997. [PubMed: 11782454]
66. Stahelin RV, Wang J, Blatner NR, Rafter JD, Murray D, Cho W. The origin of C1A-C2 interdomain interactions in protein kinase C alpha. J Biol Chem. 2005; 280:36452–36463. [PubMed: 16079140]
67. Konopatskaya O, Poole AW. Protein kinase Cα: disease regulator and therapeutic target. Trends Pharmacol Sci. 2010; 31:8–14. [PubMed: 19969380]
68. Liu Q, Molkentin JD. Protein kinase C alpha as a heart failure therapeutic target. J Mol Cell Cardiol. 2011; 51:474–478. [PubMed: 20937286]

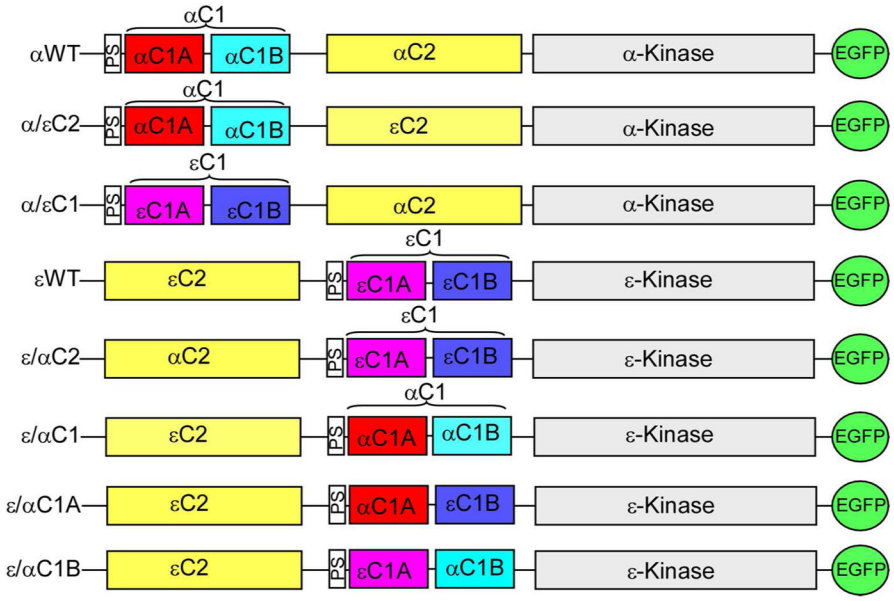

Figure 1.

Domain structure of PKCα, PKCε and their mutants. Mutants (α/εC2, α/εC1, ε/αC2, ε/αC1, ε/αC1A, and ε/αC1B) were constructed by swapping the C1 and C2 domains of PKCα (αWT) and PKCε (εWT). C1A is the first diacylglycerol/phorbol ester binding domain; C1B is the second diacylglycerol/phorbol ester binding domain; C2 is the Ca^{++} and/or phospholipid binding domain; PS is the pseudosubstrate domain and C3 and C4 are kinase domain. All constructs have enhanced green fluorescent protein (EGFP) at the C-terminus.

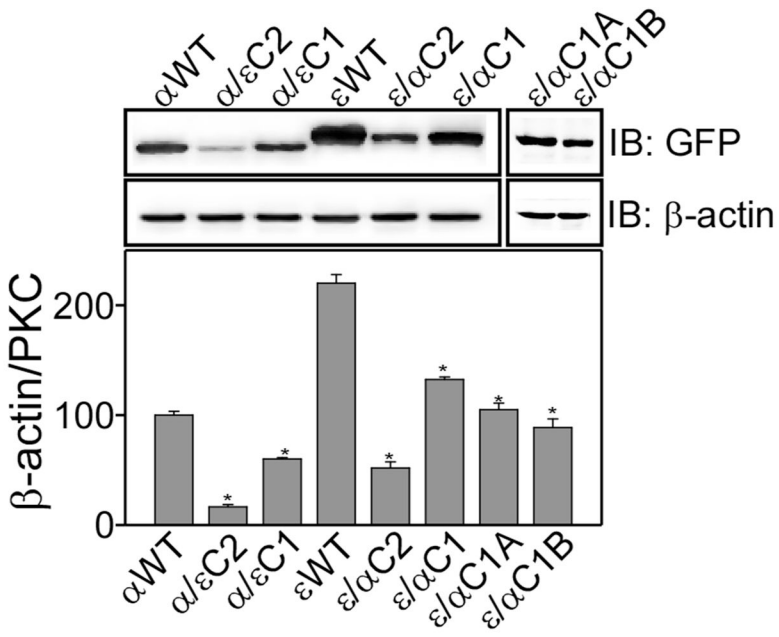

Figure 2.

Effect of domain swapping on the protein expression in HEK293 cells. Upper panel shows Western blot analysis of wild type and mutant proteins in HEK293 cells. Cells were transiently transfected with the particular plasmid, cells were lysed after 48 h and whole cell lysate (40 μg) were used for immuno-blotting. Expressed proteins were detected using anti-GFP antibody and anti-β-actin antibody was used as a loading control. The lower panel shows bar graph of densitometry analysis of the upper panel. Results are displayed as Mean ± SEM, n = 3 and one-way ANOVA (Bonferroni post hoc test) was used for statistical significance analysis. *, P values less than 0.05 were considered significant.

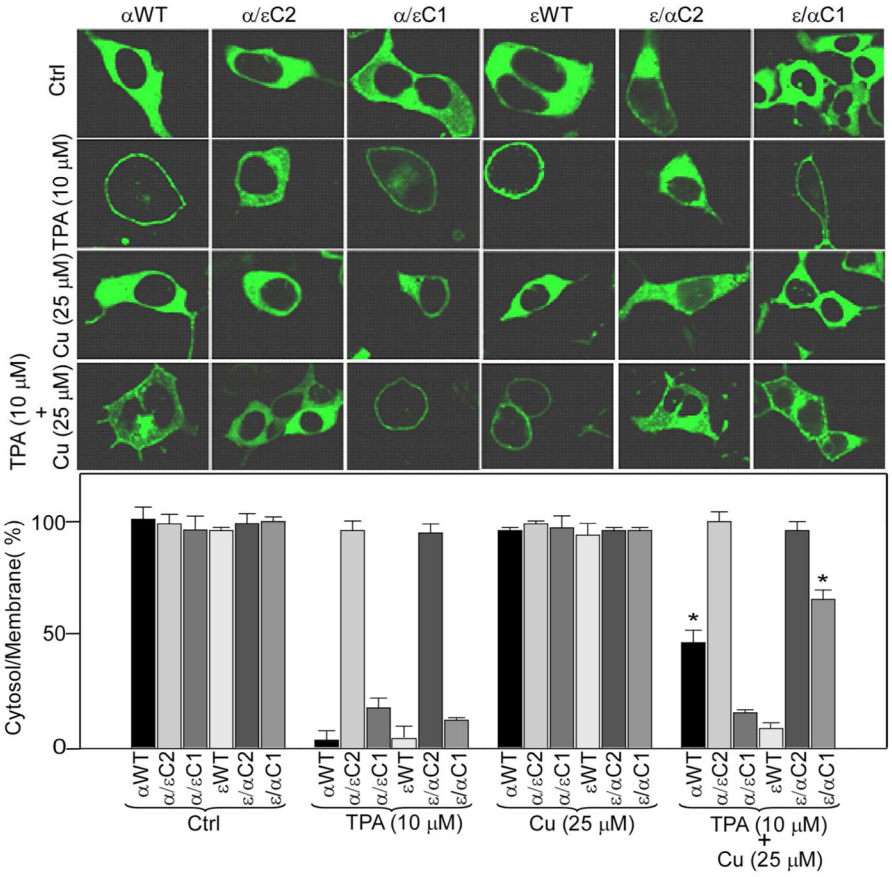

Figure 3.

Confocal analysis of the effect of curcumin on TPA-induced membrane translocation of αWT, εWT, α/εC2, α/εC1, ε/αC2 and ε/αC1. The upper panel shows the confocal images of wild type (αWT and εWT) and mutants protein (α/εC2, α/εC1, ε/αC2 and ε/αC1) after cells were treated with TPA (10 μM) and/or curcumin (25 μM) as indicated for 1 h. HEK293 cells were transiently transfected with a particular plasmid and confocal images were acquired as described in Material and Methods section. Control (ctrl) refers to the sample with vehicle (0.1% DMSO) treated cells. The lower panel bar graph shows the protein ratio of cytoplasm to plasma-membrane, quantified from fluorescence intensity. Results are displayed as Mean ± SEM derived from three independent experiments and from three different cells. One-way ANOVA (Bonferroni post hoc test) was used for statistical significance analysis. *, P values less than 0.05 are considered as significant.

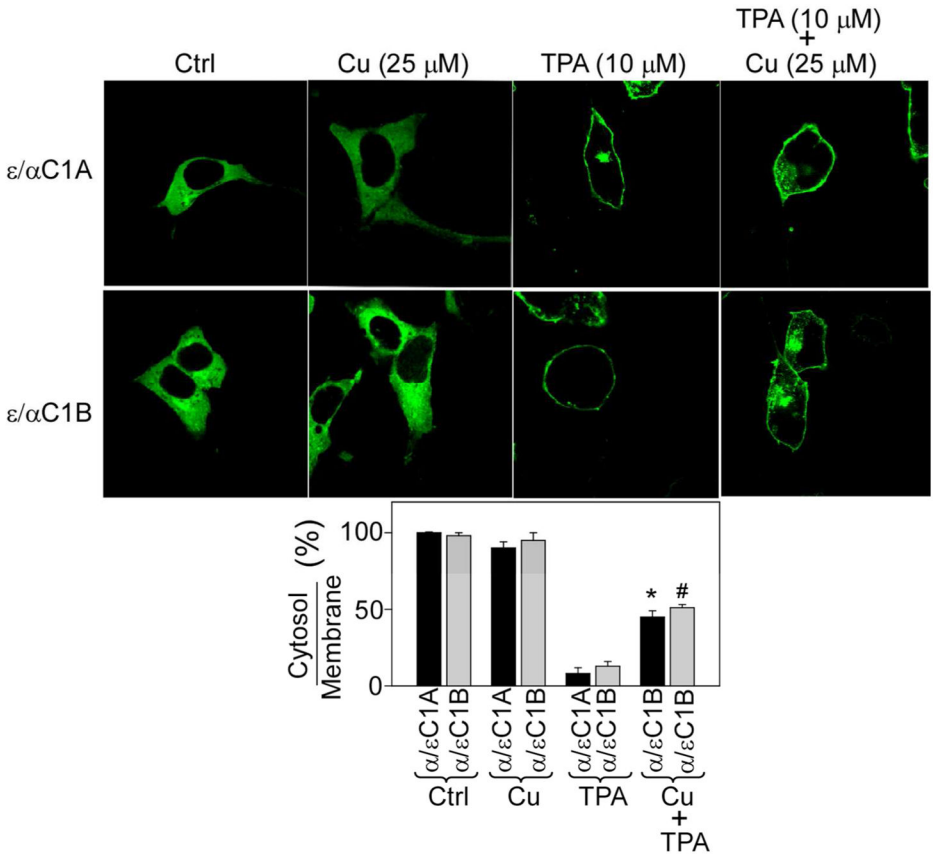

Figure 4A

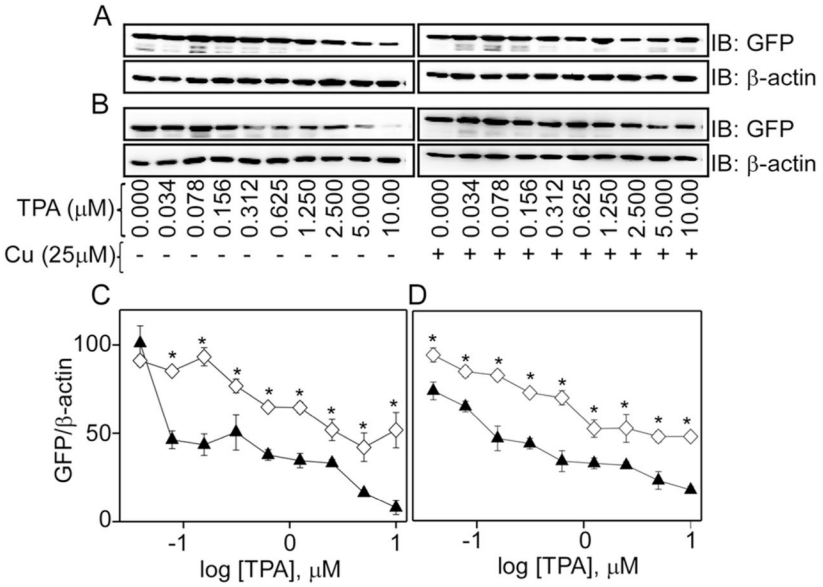

Figure 4B

Figure 4.

Figure 4A. Confocal analysis of the effect of curcumin on TPA-induced membrane translocation of ε/αC1A and ε/αC1B. The upper panel shows confocal images of ε/αC1A and ε/αC1B mutants after cells were treated with TPA (10 μM) and/or curcumin (25 μM) for 1 h. Control (ctrl) refers to the sample with vehicle (0.1% DMSO) treated cells. The lower panel bar graph shows the protein ratio of cytoplasm to plasma-membrane, quantified from fluorescence intensity of the upper panel images as described in Material and Methods section. Results are displayed as Mean ± SEM from three independent experiments and from three different cells. One-way ANOVA (Bonferroni post hoc test) was used for statistical significance analysis. *, P values less than 0.05 are considered as significant.

Figure 4B. Western blot analysis of the effect of curcumin on TPA-induced membrane translocation of the mutants, ε/αC1A and ε/αC1B. Upper panel shows Western blot analysis of cytosolic (**A**) ε/αC1A and (**B**) ε/αC1B after cells were treated with different concentration TPA (0–10 μM) (▲) and curcumin (25 μM) +TPA (◇) as indicated for 1 h. β-actin was used as a loading control. C and D in the lower panel represent the bar graph of densitometry analysis of panel **A** and **B** immuno-blots, respectively. Results are displayed as Mean ± SEM, n = 3 and one-way ANOVA (Bonferroni post hoc test) was used for statistical significance analysis. *, P values less than 0.05 are considered as significant.

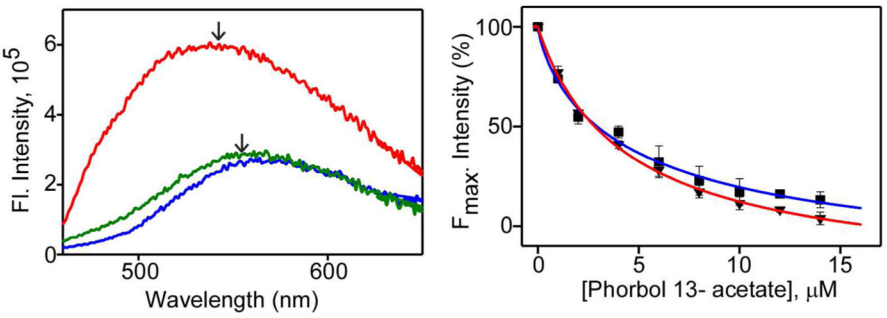

Fig 5.

Effect of phorbol 13-acetate on the binding of curcumin to αC1A and αC1B domain. Left panel, fluorescence emission spectra of curcumin (5 μM) in buffer (blue), buffer + αC1B (5 μM) (red), and buffer+ αC1B (5 μM) + TPA (10 μM) (green). Arrows indicate emission maxima. Right panel, normalized fluorescence intensity of curcumin in presence of αC1B (▼) or αC1A (■) at Em_{max} (565 nm for C1A and 552 nm for C1B) and as a function of phorbol 13-acetate concentration. IC_{50} was calculated from fitted curves using Hill equation (36) and indicated as solid lines. The IC_{50} of αC1A and αC1B were 6.27±1.2 μM and 4.47±1.7 μM respectively. Solutions were excited at 425 nm. Results are displayed as Mean ±SEM from three independent experiments.

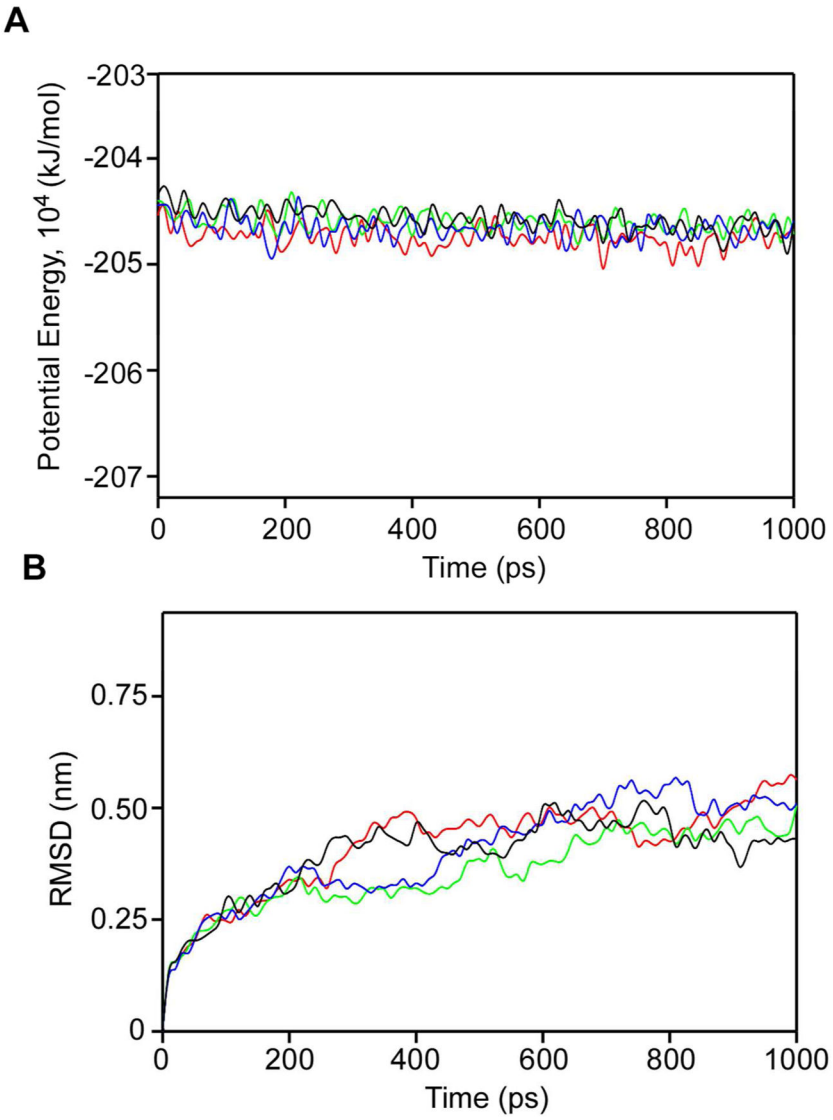

Figure 6A

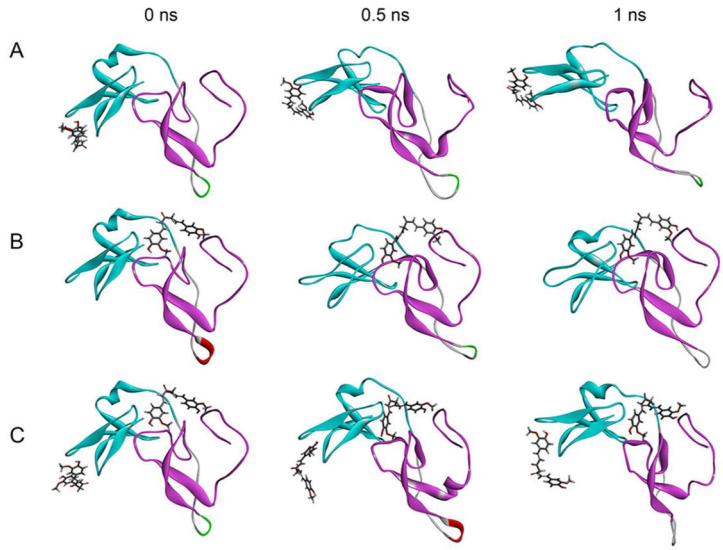

6B

Figure 6.

Fig 6A. Plots of (A) potential energy and (B) RMSD resulted from the MD simulations of free (red), curcumin docked to C1A (green), curcumin docked to C1B (black), and curcumin docked to C1A and C1B (blue) during 1.0 ns MD.

6B: Snapshots at 500 ps intervals of the MD simulations of the complexes of curcumin and the C1 (C1A+C1B) domain of PKCα. A) Curcumin docked to C1A, B) curcumin docked to C1B, and C) curcumin docked to C1A and C1B. Cyan and magenta color represents C1A and C1B domain respectively, and curcumin is represented by the line structure. The MD simulations were carried out using the GROMACS 4.6.5 package of programs.

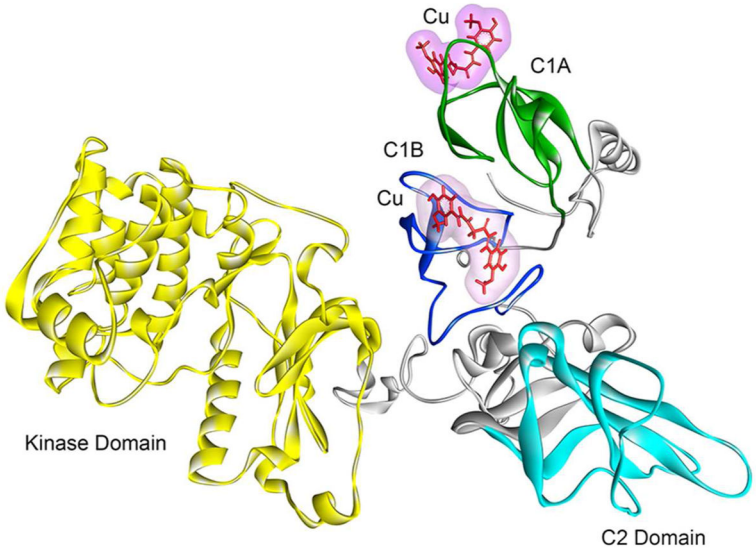

Figure 7.

Sites of interaction of curcumin in PKCα. Full-length PKCα comprising of the kinase (yellow), C1A (green), C1B (blue), and C2 (cyan) domains. Curcumin (Cu) is shown in line structure (red). The MD simulations were carried out using the GROMACS 4.6.5 package of programs.

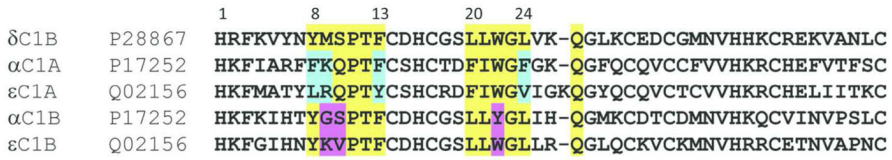

Fig 8.

Sequence comparison of the C1A and C1B sub-domains. Residues involved in the phorbol binding are highlighted in yellow. Different residues of in the C1A and C1B are highlighted in cyan and pink respectively. Structure of δC1B complexed with phorbol 13-OAc is known and the sequence of δC1B is included for highlighting the phorbol ester binding residues.